

## Aberystwyth University

### *Sequencing the Sturtian icehouse*

Busfield, M. E.; Le Heron, D. P.

*Published in:*

Journal of the Geological Society

*DOI:*

[10.1144/jgs2013-067](https://doi.org/10.1144/jgs2013-067)

*Publication date:*

2014

*Citation for published version (APA):*

Busfield, M. E., & Le Heron, D. P. (2014). Sequencing the Sturtian icehouse: Dynamic ice behaviour in South Australia. *Journal of the Geological Society*, 171(3), 443-456. <https://doi.org/10.1144/jgs2013-067>

#### **General rights**

Copyright and moral rights for the publications made accessible in the Aberystwyth Research Portal (the Institutional Repository) are retained by the authors and/or other copyright owners and it is a condition of accessing publications that users recognise and abide by the legal requirements associated with these rights.

- Users may download and print one copy of any publication from the Aberystwyth Research Portal for the purpose of private study or research.
- You may not further distribute the material or use it for any profit-making activity or commercial gain
- You may freely distribute the URL identifying the publication in the Aberystwyth Research Portal

#### **Take down policy**

If you believe that this document breaches copyright please contact us providing details, and we will remove access to the work immediately and investigate your claim.

tel: +44 1970 62 2400  
email: [is@aber.ac.uk](mailto:is@aber.ac.uk)

1                   **Sequencing the Sturtian icehouse: dynamic ice behaviour in South Australia**

2                                   M.E. BUSFIELD<sup>1\*</sup>, D.P. LE HERON<sup>1</sup>

3                   <sup>1</sup>*Department of Earth Sciences, Royal Holloway, University of London, Egham, TW20 0EX, United*  
4                                   *Kingdom*

5                                   \*Corresponding author (email: Marie.Busfield.2011@live.rhul.ac.uk)

6  
7                   **Abstract**

8                   The Cryogenian record of South Australia houses the type region of the Sturtian glaciation, the  
9                   oldest of three pan-global icehouse intervals during the Neoproterozoic. Data are presented from  
10                  previously little described sections at Holowilena Creek, Oladdie Creek and Hillpara Creek in the  
11                  central and southern Flinders Ranges, where five facies associations are recognized. These are (i)  
12                  diamictite and conglomerate, (ii) interbedded heterolithics, (iii) hummocky cross-stratified  
13                  sandstone, (iv) lonestone-bearing siltstone, and (v) ferruginous siltstone and sandstone. The  
14                  succession reveals significant lateral and vertical facies variation, which is linked to a complex  
15                  inherited palaeotopography and distance from the sediment source. Repeated stratigraphic  
16                  occurrences of striated clasts and abundant ice-rafted debris strongly support recurrent glacial  
17                  influence on sedimentation. The intercalation of gravitationally re-worked diamictites, dropstone-  
18                  bearing siltstone and dropstone-free siltstone testifies to dynamic sedimentation within a  
19                  periodically glacially-influenced subaqueous environment. Sequence stratigraphic analysis  
20                  identifies four glacial advance systems tracts (GAST), separated by three glacial retreat systems  
21                  tracts (GRST), wherein hummocky cross-stratified sandstones attest to open water conditions.  
22                  These findings support dynamic ice sheet behaviour in South Australia, and provide clear evidence  
23                  for repeated intra-Sturtian ice sheet recession.

24

25

26

## 27 **Introduction**

28 Two Neoproterozoic icehouse intervals have long been recognised in South Australia (Mawson &  
29 Sprigg, 1950), namely the older Sturtian and younger Marinoan glaciations, so named after the Sturt  
30 Gorge and Marino Rocks of Adelaide's outer suburbs (Preiss et al., 1998). The recognition of  
31 broadly age-equivalent deposits worldwide contributed to the development of the snowball Earth  
32 hypothesis (Hoffman et al., 1998; Hoffman & Schrag, 2002), wherein two distinct episodes of  
33 severe pan-global glaciation enabled ice sheets to extend to low palaeolatitudes, resulting in a  
34 suppressed hydrological cycle. Recent studies, however, support a considerably more dynamic  
35 cryosphere, with fluctuating ice margins, open water areas, and abundant evidence of hydrological  
36 activity (e.g. Etienne et al., 2007; Arnaud et al., 2011 and refs therein). Moreover, new age  
37 constraints, and their likely error bars, cast doubt on the pan-global synchronicity of these glacial  
38 events (e.g. Allen & Etienne, 2008; Condon & Bowring, 2011), and hence their two-fold  
39 subdivision as 'Sturtian' or 'Marinoan'. This holds significant bearing on the Neoproterozoic  
40 glacial deposits of South Australia, widely considered as the type area of the Sturtian icehouse  
41 period (Hoffman & Schrag, 2002).

42 The Adelaide Fold Belt of South Australia (Figs. 1-2) exposes an extremely thick succession of  
43 diamictite, sandstone and siltstone, thought to have accumulated during the Sturtian glaciation. The  
44 glacial affinity of these sediments was first proposed by Howchin (1901), arguing in favour of  
45 glaciomarine deposition (Howchin, 1908), although correlative sections were subsequently  
46 interpreted as terrestrial glacial deposits by Mawson (1941, 1949). Detailed examination of sections  
47 in the northern Flinders Ranges and Mount Painter area by Link and Gostin (1981) and Young and  
48 Gostin (1988, 1989, 1990, 1991) heralded a return to the glaciomarine hypothesis. The latter studies  
49 identify a four-fold stratigraphic subdivision, consisting of two principal diamictite units, each  
50 overlain by a succession of siltstones and sandstones, interpreted to record two glacial cycles within  
51 the Sturtian interval. The thickness of studied sections varies considerably across the region from a

52 few hundred metres, to a purported 6000 m in the Yudnamutana Trough (Fig. 2), attributed either to  
53 the development of subglacial palaeovalleys, to active extensional tectonics, or a combination of the  
54 above (Young & Gostin, 1990, 1991; Preiss, 2000).

55 Comparatively few detailed sedimentological studies have been conducted on the Sturtian deposits  
56 of the central and southern Flinders Ranges. Regional mapping identifies a major fault-bound  
57 depocentre in the Barratta Trough (Fig. 2), where Sturtian sediments attain an estimated thickness  
58 of 4000 m (Preiss, 1999, and refs therein), thinning to a few hundred metres in adjacent shelf areas  
59 (Preiss et al., 1993). Recent work by Le Heron et al. (2011a, b) at Holowilena Creek, in the central  
60 Flinders Ranges, records a thick (>800 m) succession of heterogeneous glacial strata, with  
61 abundant evidence of striated erratic clasts and ice-rafted debris (IRD). Significantly, the occurrence  
62 of dropstone-free, hummocky cross-stratified sediments punctuating the succession is interpreted as  
63 an interglacial sequence during the Sturtian interval, pointing to major ice sheet fluctuation.

64 This paper will build upon earlier work by Le Heron et al. (2011a, b) at Holowilena Creek, and  
65 present high resolution datasets for correlative sections at Oladdie Creek and Hillpara Creek,  
66 approximately 60 km further south and south-east (Fig. 1), previously described only at the  
67 reconnaissance level by Binks (1968). These sections enable the facies variability of ice-proximal to  
68 more ice-distal settings to be examined, and the influence of pre-existing topographic relief to be  
69 tested. A new sedimentary model is presented which frames the development of the diamictite-  
70 bearing successions in a glacial sequence stratigraphic context.

## 71 **Study area and stratigraphy**

72 The studied sedimentary successions belong to the mid Cryogenian Yudnamutana Subgroup, at the  
73 base of the Umberatana Group (Fig. 3). In the Adelaide Fold Belt, these sediments rest with angular  
74 unconformity upon sandstones and siltstones of the underlying Burra Group (Coats & Preiss, 1987).  
75 Stratigraphic nomenclature is highly variable across the region, but typically includes a basal

76 diamictite-dominated unit, namely the Bolla Bollana Formation to the north, the Pualco Tillite in  
77 the central regions, the Appila Tillite further south, or the Sturt Tillite in the type-section of the  
78 Adelaide Hills. These pass upwards into more heterogeneous diamictite, sandstone and siltstone  
79 facies of the Wilyerpa Formation in the central region, or the Lyndhurst Formation to the north.  
80 These deposits are in turn blanketed by the post-glacial Tindelpina Shale Member of the Tapley Hill  
81 Formation throughout the Adelaide Fold Belt (Fig. 3). Re-Os dating of the Tindelpina Shale  
82 Member provides a minimum age constraint of  $643 \pm 2.4$  Ma for the Yudnamutana Subgroup  
83 (Kendall et al., 2006), further corroborated by a U-Pb zircon date of  $659 \pm 6$  Ma derived from a  
84 volcanoclastic horizon towards the top of the Wilyerpa Formation (Fanning & Link, 2006).

85 In places, ironstone facies characterise the lower Yudnamutana Subgroup, ascribed to the  
86 Holowilena Ironstone Formation in the study area (Fig. 3), or its correlative the Braemar Ironstone  
87 Formation to the east (Forbes, 1989). The Holowilena Ironstone is variously interpreted as  
88 overlying the Pualco Tillite, (and equivalent Appila Tillite), or alternatively considered as laterally  
89 correlative (Preiss et al. 1993 and refs within). In view of this, we adopt the term ‘Holowilena  
90 Ironstone’ in reference to the distinctly ferruginous facies. The terms ‘Pualco Tillite’ and ‘Wilyerpa  
91 Formation’ will be adopted to describe the underlying and overlying sedimentary facies,  
92 respectively.

93 The study areas occur within broadly NE-SW trending outcrop belts which span the Parachilna and  
94 Orroroo map sheets (Fig. 1; Binks, 1968; Preiss, 1999). The orientation of these outcrops is  
95 considered to reflect widespread Willouran to early Sturtian rifting (c. 830 Ma - <660 Ma; Preiss et  
96 al., 2011), in this region culminating in development of the Barratta Trough depocentre (Fig. 2).

97 The studied sections to the west and south-west of this trough may thus be considered shallower  
98 ‘shelf’ deposits (Preiss et al., 1993), accumulating within neighbouring sub-basins. The sediments  
99 subsequently underwent intracratonic deformation during the Cambrian-Ordovician Delamerian  
100 Orogeny, becoming incorporated in a series of continuous, relatively upright fold structures at the

101 northern margin of the Nackara Arc (Preiss, 2000). The rocks of the study area are characterised by  
102 low grade, greenschist facies metamorphism (Preiss, 1995). The minimal metamorphic overprint  
103 thus permits detailed study of primary sedimentary facies and structures.

#### 104 **Facies analysis**

105 Data are presented from three detailed logged sections at Holowilena Creek, Oladdie Creek and  
106 Hillpara Creek (Fig. 4). Exposure of the underlying Burra Group sediments permits regional  
107 correlation, whereas the overlying Tapley Hill Formation is only recorded at Oladdie Creek.  
108 Therefore, only minimum thicknesses are observed at Holowilena and Hillpara Creeks, although  
109 considerable thickness variations across the logged sections are demonstrable by correlation. Five  
110 facies associations are recognized, namely (i) diamictite and conglomerate, (ii) interbedded  
111 heterolithic, (iii) hummocky cross-stratified sandstone, (iv) lonestone-bearing siltstone, and (v)  
112 ferruginous siltstone and sandstone.

#### 113 *Diamictite and conglomerate facies association*

114 This facies association makes up almost the entire section at Hillpara Creek, is notably dominant at  
115 Oladdie Creek, and constitutes less than 50% of the succession at Holowilena Creek. It is sandy  
116 throughout, and predominantly crudely stratified, with subsidiary massive and well stratified  
117 varieties. The conglomerate deposits commonly display normal grading, fining into diamictite  
118 deposits, whilst the latter include normal, reverse and non-graded varieties (Fig. 4). Erosive contacts  
119 are prevalent at the base of conglomerates and clast-rich diamictites (Fig. 5a). Outsized clasts range  
120 from c. 3-80 cm in size, typically 15-20 cm, and comprise limestone, dolostone, metasediments,  
121 basalt and granite. Clasts are predominantly sub-angular to sub-rounded in shape; striated forms  
122 locally occur.

123 Downwarping and puncturing of laminae beneath pebble to boulder sized clasts is common (Fig.  
124 5b, c), particularly in the crudely stratified diamictites. Other oversized clasts frequently form turbate  
125 structures, where smaller clasts form circular alignments around a core stone or rigid matrix (Fig.  
126 5d, e), and are especially common where downwarping structures are rare. Lenticular siltstone and  
127 sandstone bodies locally occur, and are typically bed-parallel. However in places these lenses are  
128 highly deformed, forming tight to recumbent intrabed fold structures.

129 *Interpretation.* The diamictite and conglomerate facies association is interpreted as a series of  
130 glacially-influenced, subaqueous sediment flow deposits. The common fining-upward motif and  
131 internal organisation of stacked conglomerate and diamictite deposits is typical of turbulence within  
132 the flow (Talling et al. 2012), representing high-density and more dilute turbidites, respectively.  
133 This is supported by the abundance of turbate structures, attributed to the generation of transient  
134 rotational eddies during turbulent flow (Phillips, 2006). Similar structures can be generated during  
135 subglacial shearing of diamictites (e.g. Busfield & Le Heron 2013, and refs within), but this  
136 interpretation is deemed unlikely in the absence of other shear-related features e.g. attenuated clasts,  
137 pressure shadows, galaxy structures. Massive and reverse graded diamictite deposits are interpreted  
138 as the product of glaciogenic debris flows (GDFs), which commonly generate inverse grading  
139 patterns through the combined influence of upward clast migration and kinetic sieving (Legros,  
140 2002; Benn & Evans, 2010; Talling et al., 2012). Erosive contacts at the base of many conglomerate  
141 and clast-rich diamictite units reflects repeated sediment flow emplacement, and resultant  
142 cannibalisation of underlying sediments.

143 The close association of GDFs and turbidites likely reflects flow transformation during downslope  
144 movement, whereby mixing of the subaqueous debris flow with the overlying water body results in  
145 flow dilution (Benn & Evans, 2010; Talling et al., 2012), and hence a tendency towards more  
146 turbulent flow conditions. The generation of these 'linked' turbidity currents frequently occurs  
147 through transformation of moderate strength debris flows (Talling et al., 2012), and is a common

148 process within ice-proximal and ice-contact regimes under rates of high sedimentation (Benn &  
149 Evans, 2010). This is consistent with the occurrence of tight to recumbent folded sand lenses,  
150 associated with slumping and sediment failure in response to rapid sediment delivery (Maltman,  
151 1994). Outsized clasts which downwarp and puncture underlying laminae are interpreted as ice-  
152 rafted debris (IRD), wherein the preserved examples likely accumulated as sediment flows waned,  
153 thus restricting overprint of the structures under downslope remobilisation. The local occurrences of  
154 striated clasts provide further credence to the proposed glacial origin.

#### 155 *Interbedded heterolithic facies association*

156 This facies association comprises a series of well stratified, dominantly interbedded siltstones, fine  
157 sandstones and coarse quartz arenites. It is most prominent in the Holowilena Creek section,  
158 constituting approximately 30% of the succession, diminishing to <10% in the Oladdie Creek  
159 deposits and c. 2% at Hillpara Creek (Fig. 4). No lonestones occur within this facies association.  
160 The deposits exhibit minimal grading; rarely sandstone interbeds fine upward into the overlying  
161 siltstone. Current ripple cross-lamination is common within the fine sandstone-siltstone interbeds  
162 (Fig. 6a), predominantly demonstrating palaeoflow towards the north. An isolated example of  
163 climbing ripple cross-lamination is recorded at Oladdie Creek. In places, the fine sandstone  
164 interbeds are deformed into largely bed-parallel discontinuous fold structures (Fig. 6b), other beds  
165 contain highly convolute lamination as well as load and flame structures (Fig. 6c). Conversely, the  
166 coarser quartzite interbeds are planar throughout, and exhibit no sedimentary structures at  
167 Holowilena or Oladdie, with limited evidence of small-pebble lined cross-bedding in the Hillpara  
168 Creek section (at ~75 m Log C, Fig. 4).

169 *Interpretation.* The interbedded heterolithic facies association is interpreted as a finer grained  
170 series of sediment flow deposits, wherein the enhanced preservation of bedforms likely reflects  
171 reduced sediment concentrations compared to the coarser diamictite and conglomerate facies



172 association. This may be a product of diminished sediment supply, which in tandem with the loss of  
173 the ice-rafting signature can be used to support periods of relative ice margin stability or retreat  
174 during deposition of the interbedded heterolithics. Within the coarser grained diamictite and  
175 conglomerate facies association, higher sediment concentrations and fall-out rates suppress the  
176 migration and preservation of delicate ripple structures (Sumner et al., 2008; Talling et al., 2012).  
177 However, as they move downslope, flows become more dilute through mixing with the water  
178 column, generating fully turbulent, low-density flows that enable the development of ripple cross-  
179 lamination (Baas et al., 2011; Talling et al., 2012). Rare normally-graded sandstone interbeds are  
180 likewise interpreted to record deposition from turbulent underflows, succeeded by settling of  
181 hemipelagic silt material as the flows waned (e.g. Allen et al., 2004). The preservation of convolute  
182 lamination and climbing ripple cross-lamination at intervals reflects periods of more rapid turbidite  
183 deposition (Kuenen & Humbert, 1969; Allen, 1991; Baas, 2000; Jobe et al., 2012; Talling et al.,  
184 2012). Similarly, folded sandstone and siltstone beds/lenses attest to downslope slumping and  
185 sediment instability induced by rapid sedimentation (Maltman, 1994). Load and flame structures  
186 attest to Rayleigh-Taylor instabilities initiated at a grain-size/bed interface (Allen, 1984; Collinson  
187 and Thompson, 1987).

188 The coarser quartz arenite beds typically lack internal organisation, and are thus interpreted as non-  
189 or poorly-cohesive, clean sand debrites (Talling et al., 2012). An alternative mechanism of  
190 incremental accumulation via high-density turbidity currents is rejected owing to the absence of  
191 vertical and lateral grading (Kneller & Branney, 1995; Talling et al., 2012). Moreover, the  
192 prominent cross-bedded quartzite bed at Hillpara Creek (at ~75 m Log C, Fig. 4) pinches out  
193 sharply as opposed to gradationally, considered a characteristic feature of debris flow deposition  
194 (Johnson, 1970; Major & Iverson, 1999; Amy et al., 2005; Amy & Talling, 2006). The generation  
195 of dune-scale traction bedforms is also incompatible with rapid deposition from a high-density  
196 turbidity current (Kuenen, 1966; Middleton & Hampton, 1973; Talling et al., 2012). The prominent

197 quartzite bed at Hillpara has been previously interpreted as a large ice-rafted erratic (Binks, 1968).  
198 However, in light of its bed-parallel orientation, the absence of associated impact-related  
199 deformation and its textural similarity to other quartzite interbeds at Holowilena and Oladdie, we  
200 prefer interpretation as a laterally discontinuous debrite.

201 *Hummocky cross-stratified sandstone facies association*

202 This facies association is restricted to the Holowilena Creek section (Log A, Fig. 4). Overall, the  
203 facies resemble those of the interbedded heterolithic facies association in that they comprise well  
204 stratified, non-graded fine sandstone and siltstone interbeds. They are distinguished, however, by  
205 the occurrence of hummocky cross-stratification (HCS) within many of the sandstone units (Fig.  
206 6d-e). The bedforms are predominantly isotropic, with subsidiary anisotropic components. Current  
207 ripple cross-laminated and convolute laminated sandstones are also intercalated within this facies  
208 association. Lonestones were not observed.

209 *Interpretation.* The interbedded current rippled sandstones and laminated siltstones are interpreted  
210 to record turbulent underflow deposition and settling of hemipelagic fines, respectively, in concert  
211 with the interbedded heterolithic facies association. However, the presence of HCS attests to the  
212 interplay of storm wave oscillatory flow during deposition, within a shallow shelf environment  
213 (Cheel & Leckie, 1993; Johnson & Baldwin, 1996; Duke et al., 1991; Dumas & Arnott, 2006). Le  
214 Heron et al. (2011a, b) argue in favour of sea ice-free conditions at this time, as sea ice would  
215 inhibit the efficacy of storm wave agitation. Certainly these features attest to a sea ice minimum  
216 zone, where sufficient expanses of open water enable storm wave agitation, although the extent of  
217 ice meltback remains unclear. The absence of lonestones within this facies association is consistent  
218 with a lack of glacial influence on deposition.

219 *Lonestone-bearing siltstone facies association*

220 This facies association consists predominantly of planar laminated siltstone, with notably fewer  
221 sandstone beds than the interbedded heterolithic facies association. It is restricted to the  
222 Holowilena and Oladdie Creek sections, constituting <10% and <5% of the succession, respectively  
223 (Fig. 4). Downwarping of laminae beneath the oversized limestones is common, in places piercing  
224 the laminae also (Fig. 6f). Rarely, lamina-parallel trains of limestones are recorded, coincident with  
225 the absence of downwarping features.

226 *Interpretation.* The predominance of planar laminated siltstone alongside minor sandstone interbeds  
227 is interpreted to record settling of hemipelagic fines, interrupted by isolated sand-rich sediment  
228 underflows. The presence of oversized limestones which puncture and downwarp underlying laminae  
229 provides clear evidence of ice-rafting during deposition. Sediment flow 'rafting' of the limestones  
230 (e.g. Postma et al., 1988; Eyles & Januszczak, 2007) is discounted on the basis of the fine grain size  
231 of the supporting material, which would lack the cohesive strength to transport cobble to boulder  
232 sized material.

### 233 *Ferruginous siltstone and sandstone facies association*

234 This facies association is again restricted to Holowilena Creek, and attains only 6 m in thickness in  
235 the studied section (Log A, Fig. 4). It comprises both massive and crudely stratified fine sandstone  
236 and siltstone, with few granule to small pebble sized clasts, which are locally associated with  
237 impact-related deformation at the micro-scale (Fig. 6g). No pebble or boulder sized limestones were  
238 observed within this facies association. Sharp, undulose, bed-parallel layering is apparent in the  
239 siltstone unit (Fig. 6h), alongside an isolated asymmetric fold structure verging towards the south-  
240 east (Fig. 6i).

241 *Interpretation.* The ferruginous siltstone and sandstone facies association is tentatively interpreted  
242 to record similar styles of hemipelagic silt deposition and underflow sand emplacement as the  
243 limestone bearing siltstone facies association. However, impact-related deformation beneath granule

244 sized clasts at the micro-scale is interpreted to record early onset of ice-rafting processes. It is  
245 possible that the bed-parallel, undulose layering (Fig. 6h) may represent horizontal algal laminites,  
246 and by association an algal growth structure preserved in the asymmetric fold. This tentative  
247 interpretation is based on recognition of similar features observed in age-equivalent deposits of  
248 northern Namibia (Le Heron et al., 2013), but requires further investigation.

249 The source of iron minerals within Neoproterozoic glacial successions remains highly contentious,  
250 and is considered beyond the scope of this study given its limited outcrop occurrence. Recent  
251 studies in South Australia support the intermixing of detrital terrestrial sediment and hydrothermal  
252 fluids (Lottermoser & Ashley, 2000; Cox et al., in press). In contrast to previous studies which  
253 advocate globally-widespread seawater anoxia (e.g. Kirschvink, 1992), the accumulation of  
254 abundant soluble iron, and hence deposition of iron-enriched sediments, is thought to occur under  
255 enhanced, not extreme anoxia and elevated Fe:S ratios (Cox et al., in press).

### 256 **Depositional cycles and glacial sequence stratigraphy**

257 The preceding facies analysis reveals a diverse accumulation of sediments both with and without  
258 evidence of glacial influence on deposition. Examination of the vertical grading of these facies  
259 associations, alongside changes in their lateral distribution, provides insight into their depositional  
260 history, and enables a sequence stratigraphic framework to be constructed. Sequence stratigraphic  
261 concepts are scarcely applied to glacial depositional systems (e.g. Proust & Deynoux, 1994;  
262 Brookfield & Martini, 1999; Powell & Cooper, 2002; El-ghali, 2005; Pedersen, 2012), largely due  
263 to the complexity of deciphering the influence of glacial fluctuations from changes in relative  
264 lake/sea-level. The term 'glacial sequence stratigraphy' is therefore used to denote a sequence  
265 stratigraphic model driven by glacier dynamics (Powell & Cooper, 2002), the effects of which are  
266 preserved independently of other external forces e.g. eustasy, isostasy. Glacial systems tracts (GST)  
267 are defined following the scheme of Powell & Cooper (2002). Systems tracts are subdivided into

268 glacial advance (GAST) and glacial retreat (GRST) sequences, which may also include ice  
269 maximum (GMaST) and ice minimum (GMiST) conditions, respectively. Ten glacial systems tracts  
270 are recognized (Fig. 7), separated either by a glacial erosion surface (GES) or glacial bounding  
271 surface (GBS), the latter including the glacial advance surface (GAS) representing the onset of  
272 advance systems tracts, and the iceberg-rafting termination surface (ITS) representing the onset of  
273 retreat.

274 The first sequence is restricted to the base of the Holowilena Creek section (Fig. 7), and constitutes  
275 striated clast-bearing sediment gravity flow deposits of the diamictite and conglomerate facies  
276 association, correlated to the Pualco Tillite. This sequence is attributed to the glacial advance  
277 systems tract (GAST 1) due to its characteristically thin exposure, and coarsening-upward motif  
278 (Powell & Cooper, 2002). The sequence is capped by an onlap surface, representing the first glacial  
279 bounding surface (*GBS1*), beneath sediments of the interbedded heterolithics facies association  
280 (Fig. 8a). This onlap surface is interpreted to reflect transgression following local ice meltback,  
281 demarcating the base of the first glacial retreat systems tract (GRST 1), consistent with the absence  
282 of glacial indicators (e.g. IRD) in the overlying heterolithic facies (Fig. 7). These sediments are  
283 overlain by the ferruginous siltstone and sandstone facies association, the Holowilena Ironstone.  
284 The first appearance of micro-scale IRD at this interval is interpreted as the glacial advance surface  
285 (*GAS1*; Powell & Cooper, 2002), and thus the overlying Holowilena Ironstone is interpreted as a  
286 thinly exposed remnant of the second GAST.

287 The top of the Holowilena Ironstone is sharply truncated by a glacial erosion surface (*GES1*) in the  
288 Holowilena Creek section (Figs. 7 & 8b); a widely recognized disconformity throughout the  
289 Flinders Ranges (e.g. Coats, 1981; Preiss et al. 1993). The thin exposure of the underlying GAST 2  
290 likely reflects significant downcutting during development of the GES. The surface is correlated to  
291 the top of the pre-glacial Burra Group sediments at Oladdie Creek and Hillpara Creek based upon  
292 the absence of the underlying Pualco Tillite and Holowilena Ironstone, although no significant

293 erosion surface was observed. The absence of a significant erosion surface in the proximal sections  
294 is likely attributed to re-working and erosion during subsequent sediment flow emplacement (during  
295 GRST 2), as opposed to marine ravinement, the effects of which would be expected to be more  
296 prominent in the distal sections, and accompanied by a transgressive lag, which is not present.  
297 Deposits of the glacial maximum systems tract (GMaST) are not recorded above the GES, as is  
298 typical of many temperate glacial systems (Powell & Cooper, 2002). Instead, at Holowilena and  
299 Oladdie, the overlying sediments of the Wilyerpa Formation correspond to a second phase of glacial  
300 retreat (GRST 2, Fig. 7). These comprise stacked, dominantly fining-upward deposits of the  
301 diamictite and conglomerate facies association and interbedded heterolithics facies association. The  
302 former contains repeated intervals of IRD, which are typically absent in the latter. This is  
303 interpreted as the product of pulsed collapse events at the ice front, driving coarser grained gravity  
304 flows and iceberg distribution into the basin, followed by periods of relative ice margin stability or  
305 retreat. During these intervals, the shelf becomes starved of coarser sediment, leading to deposition  
306 of finer grained sediment flow deposits, and ice-rafting processes are inhibited.

307 Transition to an advance systems tract (GAST 3) is recorded above this sequence (at *GBS2*, Fig. 7),  
308 where coarser grained sediments of the diamictite and conglomerate facies association pre-  
309 dominate, concomitant with a switch to a coarsening-upward motif. A pronounced inverse-grading  
310 event can be correlated across all three logged sections (Fig. 7: 260 m Log A, 62 m Log B, 18 m  
311 Log C), and at Holowilena is accompanied by a sudden influx of exotic pebble to boulder sized  
312 granite clasts (Fig. 8c). This event is interpreted to record ice maximum conditions (GMaST),  
313 resulting in high rates of sediment supply and delivery of extrabasinal erratic lithologies. At  
314 Holowilena and Oladdie a thin succession of normally-graded diamictite and conglomerate facies  
315 above *GBS3* mark a return of the GRST (3), capped by an abrupt facies dislocation to thinly  
316 laminated siltstones (Fig. 7). This facies change is concurrent with the disappearance of IRD, and is  
317 thus identified as the iceberg-rafting termination surface (*ITS1*; Powell & Cooper, 2002).

318 The retreat sequence above *ITS1* is largely restricted to the Holowilena Creek section (Fig. 7), and  
319 comprises the hummocky cross-stratified sandstone facies association at the base, and interbedded  
320 heterolithic facies association above. The occurrence of hummocky cross-stratification in the basal  
321 sediments, requiring sufficient open waters and hence sea ice meltback to permit storm wave  
322 agitation (Le Heron et al. 2011a, b), is used to support ice minimum conditions (GMiST).  
323 Moreover, HCS is typically encountered within a shallow shelf setting (Cheel & Leckie, 1993;  
324 Johnson & Baldwin, 1996; Duke et al., 1991; Dumas & Arnott, 2006), and thus the absence of this  
325 facies association in the more proximal, shallower Oladdie Creek and Hillpara Creek sections may  
326 reflect a period of subaerial exposure and non-deposition in the proximal reaches during this retreat  
327 phase. The overlying interbedded heterolithic facies above *GBS4* record an influx of coarser grained  
328 sand underflows within the Oladdie and Holowilena Creek sections, interpreted as the product of  
329 increased sediment instability in the source region, perhaps in response to initial, more proximal ice  
330 movement which may correspond to early GAST. However, the first appearance of IRD in the  
331 overlying laminated siltstones is taken as a more reliable indicator of initial advance (Powell &  
332 Cooper, 2002), identified as the second glacial advance surface (*GAS2*; Fig. 7).

333 The overlying GAST 4 is initially characterised by stacked, thickly-bedded IRD-bearing diamictite  
334 and conglomerate at Hillpara Creek, normally-graded and thinly bedded diamictite and  
335 conglomerate separated by IRD-bearing siltstone at Oladdie Creek, and by IRD-bearing siltstone  
336 only at Holowilena Creek (Fig. 7). These facies associations reflect initial advance of the ice front,  
337 where coarse-grained glacially-influenced sediment flows are deposited in the more proximal  
338 regions (Hillpara), further downslope these sediment flows occur as pulsed events separated by  
339 periods of quiescence where ice-rafting processes dominate (Oladdie), and the distal regions remain  
340 starved of coarser-grained sediment, preserving only the ice-rafting signature (Holowilena).  
341 Towards the top of the succession, above *GBS5*, thickly-bedded and dominantly inverse graded

342 diamictites, conglomerates and coarse-grained sandstones are preserved across all three logged  
343 sections, reflecting full glacial advance during late stage GAST 4, identified as the GMaST (Fig. 7).

344 The upper contact of the Wilyerpa Formation, and cessation of glacially-influenced sedimentation,  
345 was observed only in the Oladdie Creek section (Fig. 7). Here, an erosional contact occurs at the  
346 base of a pebble to boulder-bearing conglomerate, with a distinct dark grey silt matrix, notably  
347 dissimilar to the pale brown sandy matrix of the underlying Wilyerpa Formation (Fig. 8d). The  
348 conglomerate is interpreted as a post-glacial transgressive lag, and is succeeded by a thick  
349 succession of laminated dark grey siltstones of the Tindelpina Shale Member, the basal unit of the  
350 Tapley Hill Formation.

## 351 **Discussion**

352 Sequence stratigraphic analysis of the studied sections in the central and southern Flinders Ranges  
353 identifies four distinct glacial advance sequences, separated by three intervals of ice meltback (Fig.  
354 7). The glacial influence on deposition (IRD) is pervasive throughout the Hillpara and Oladdie  
355 Creek sections. This is consistent with their more proximal position relative to the ice front (see Fig.  
356 9), corroborated by the predominance of coarser grained facies associations, as well as ripple cross-  
357 lamination and soft sediment slump folding indicative of sediment supply from the south. The  
358 Holowilena Creek section represents the most ice-distal position, as indicated by the clear increase  
359 of fine grained facies. Deposition in the ice-proximal zone is proposed due to the dominance of  
360 sediment gravity flow and ice-rafting processes (Benn & Evans, 2010), with sediment accumulation  
361 on the shelf at Hillpara and Oladdie, and the slope at Holowilena (Fig. 9).

362 The studied sections demonstrate considerable thickness variations, thickening by a few tens of  
363 metres from Hillpara to Oladdie, and by several hundred metres to Holowilena Creek (Fig. 7). This  
364 is attributed to significant palaeotopographic relief during deposition (see Fig. 9), the origin of  
365 which remains obscure. Previous studies have advocated accumulation of Sturtian glacial



366 sediments within pre- and early syn-depositional rift basins (e.g. Preiss, 2000), whilst the presence  
367 of a distinct glacial erosion surface immediately above the Holowilena Ironstone may be used to  
368 support the interplay of subglacial downcutting (*sensu* Young & Gostin, 1990, 1991). Nonetheless,  
369 the palaeotopographic depression at Holowilena provided enhanced accommodation space for the  
370 preservation of non-glacially influenced regressive systems tracts, alongside protection from  
371 cannibalization under repeated sediment flow emplacement. In contrast, on the palaeotopographic  
372 highs at Oladdie and Hillpara (Fig. 9), relatively thin successions of stacked coarse-grained  
373 sediment flows likely underwent significant cannibalization and re-working during subsequent  
374 downslope movements, re-deposited basinward as flows waned, and hence glacial advance systems  
375 tracts are preferentially preserved.

376 Previous studies in South Australia have also identified multiple advance-retreat sequences within  
377 the Sturtian record (e.g. Forbes, 1970; Forbes & Cooper, 1976; Coats & Preiss, 1987; Young &  
378 Gostin 1988, 1989, 1990, 1991; Le Heron et al., 2011b). The four-fold stratigraphic subdivision of  
379 Young & Gostin (1990, 1991) comprises two diamictite-dominated intervals, each overlain by  
380 mudstone-dominated facies, interpreted as glacial advance and retreat sequences, respectively. The  
381 uppermost mudstone-dominated interval, Unit 4 of Young & Gostin (1990), is regarded as a  
382 transitional unit between the diamictic deposits of Unit 3 and the shale-rich deposits of the post-  
383 glacial Tapley Hill Formation. These considerations suggest the diamictites of the upper GMaST in  
384 the central and southern Flinders Ranges, overlain by the Tapley Hill Formation at Oladdie Creek  
385 (Fig. 7), correlate with Unit 3 of Young & Gostin (1990, 1991), and therefore Unit 4 is absent. The  
386 absence of Unit 4 from sequences in the Northern Flinders Basin (Young & Gostin, 1990) is  
387 attributed to non-deposition on topographically elevated regions, possibly in response to local  
388 tectonic and/or isostatic readjustments. This is considered plausible following the significant glacial  
389 advance recorded in the upper GMaST (this study) and Unit 3 (Young & Gostin, 1990, 1991).  
390 Furthermore, the basal GAST 1 and GRST 1 identified in the Holowilena Creek section are not

391 recorded by Young & Gostin (1990, 1991). Previous studies in the Olary region to the east of the  
392 Orroroo map sheet, however, also recognize the basal Pualco Tillite as recording the glacial  
393 maximum of the first Sturtian glaciation (Forbes, 1989; Coats & Preiss, 1987). The absence of these  
394 depositional sequences in the Northern Flinders Basin may reflect erosion during subglacial  
395 downcutting, coeval with GES 1 at the top of the Holowilena Ironstone (Figs. 7-9).

396 In the North Flinders Basin, Le Heron et al. (in press) recently interpreted a trough mouth fan  
397 (TMF) in the Sturtian glaciogenic record, building out seaward of a small palaeo-ice stream. Three  
398 facies associations are recognized, comprising a diamictite facies association accumulating via  
399 glaciogenic debris flows and ice-rafting processes at the ice margin, a channel belt facies  
400 association recording channelized turbidity currents subject to ice-rafting on the proximal and  
401 medial areas of the fan, and a sheet heterolithic facies association, deposited as non-channelized  
402 turbidites and ice-rafted debris. The overriding signature of sediment gravity flow deposition  
403 subject to ice-rafting processes closely mirrors the depositional sequences described in this study.  
404 The sequences are readily differentiated, however, on the abundance of coarse-grained material.  
405 The Bolla Bollana Formation (Le Heron et al. in press) is dominated by coarse grained diamictite  
406 and conglomerate facies, with a subordinate fines component throughout, and hence records  
407 deposition principally as sediment concentrated glaciogenic debris flows (GDFs). Our present  
408 study, meanwhile, demonstrates significantly greater facies variability, a more diverse range of  
409 grain sizes throughout, and a notably more abundant component of fines. As a result, the dominant  
410 mode of deposition is via less concentrated turbulent sediment flows. Le Heron et al. (in press)  
411 correlated the Bolla Bollana Formation to the second glacial advance (Unit 3) of Young & Gostin  
412 (1991), which would therefore equate to the upper GMaST of this study. This is consistent with  
413 build-out of TMFs during glacial advance (e.g. Powell & Cooper, 2002; Ó' Cofaigh et al., 2012).  
414 The North Flinders Basin is, however, widely considered as a separate sub-basin, disconnected from  
415 the depocentres of the central and southern Flinders Ranges (Preiss 1987, 2000; Preiss et al. 2011).

416 Arguably, therefore, separate ice masses may have fed each depocentre, where the evidence for  
417 concomitant advance phases, each following a period of significant ice meltback, may testify to  
418 regional warming and cooling events.

419 To summarise, this study proposes multiple, clear-cut cycles within the Sturtian glaciation of South  
420 Australia. Whilst the concept of hydrological shutdown under the snowball Earth hypothesis  
421 (Hoffman et al., 1998; Hoffman & Schrag, 2002) is readily dismissed from sedimentological  
422 evidence (Allen and Etienne, 2008), the true nature of ice sheet dynamics have awaited  
423 clarification. Despite having received very few attempts to apply it in the Cryogenian, sequence  
424 stratigraphic analysis is clearly a valuable tool to elucidate glacial cycles, including recognition of  
425 open water during glacial minima. Detailed examination of the sections at Holowilena Creek,  
426 Oladdie Creek and Hillpara Creek therefore contribute to the growing body of research supporting a  
427 dynamic Neoproterozoic cryosphere, akin to the numerous Phanerozoic icehouse events recorded  
428 throughout Earth's history (e.g. Etienne et al., 2007; Allen & Etienne, 2008; Arnaud et al., 2011 and  
429 refs therein). Contingent on an adequate chronostratigraphic framework, detailed facies and  
430 sequence stratigraphic analysis of pan-global 'Sturtian' successions may even allow the  
431 glaciodynamic signature of these successions to be assessed on a global scale.

## 432 **Conclusions**

433 Detailed sedimentary logging of previously little described sections in Holowilena Creek, Oladdie  
434 Creek and Hillpara Creek in the central and southern Flinders Ranges reveals significant lateral and  
435 vertical facies variation within the Yudnamutana Subgroup. Repeated occurrences of ice-rafted  
436 debris and subglacially striated clasts attest to a strong glacial influence on sedimentation. The  
437 application of glacial sequence stratigraphy enables the dynamics of the Sturtian ice sheet to be  
438 elucidated:

- 439 • Five facies associations are recognized: 1) Diamictite and conglomerate facies association  
440 (glaciogenic debris flows and turbidites subject to secondary ice-rafting), 2) Interbedded  
441 heterolithic facies association (debrites, low-density turbidites and hemipelagic fines), 3)  
442 Hummocky cross-stratified sandstone facies association (storm-wave agitation of low-  
443 density turbidity currents and settling of hemipelagic fines), 4) Lonestone-bearing siltstone  
444 facies association (settling of hemipelagic fines and isolated sand-rich turbulent  
445 underflows), and 5) Ferruginous siltstone and sandstone facies association (settling of  
446 hemipelagic fines and sand-rich turbulent underflows under enhanced anoxia, subject to  
447 subordinate ice-rafting).
- 448 • Thickness variations across the logged sections attest to an irregular underlying  
449 palaeotopography during deposition, attributed to the combined influence of pre- and early  
450 syn-depositional rift activity and subglacial downcutting.
- 451 • Glacial sequence stratigraphic analysis identifies four glacial advance systems tracts  
452 (GAST), separated by three glacial retreat systems tracts (GRST), the uppermost GRST 3  
453 testifying to open water conditions. These findings support dynamic advance and retreat of  
454 the Sturtian ice sheet, requiring an active hydrological cycle.

#### 455 **Acknowledgements**

456 The authors are extremely grateful to Alan S Collins (University of Adelaide) and Benjamin L  
457 Moorhouse (University of Otago) for their assistance in the field. We would like to thank the two  
458 anonymous reviewers for suggestions which allowed us to improve the manuscript, Anthony  
459 Spencer for constructive comments on an earlier draft of the manuscript, and the editorial input of  
460 Philip Hughes. This work was funded by the National Geographic Explorer Fund, Novas  
461 Consulting Research Grant (Geological Society, London), Gill Harwood Memorial Fund (BSRG)  
462 and the Helen Shackleton Award (RHUL).

463 **References**

- 464 ALLEN, J.R.L. 1984. *Sedimentary Structures: Their Character and Physical Basis, volumes I and*  
465 *II*. Elsevier, Amsterdam, 593 p.
- 466 ALLEN, J.R.L. 1991. The Bouma A division and the possible duration of turbidity currents.  
467 *Journal of Sedimentary Petrology*, **61**, 291-295.
- 468 ALLEN, P.A. & ETIENNE, J.L. 2008. Sedimentary challenge to Snowball Earth. *Nature*  
469 *Geoscience*, **1**, 817-825.
- 470 ALLEN, P.A., LEATHER, J. & BRASIER, M.D. 2004. The Neoproterozoic Fiq glaciation and its  
471 aftermath, Huqf supergroup of Oman. *Basin Research*, **16**, 507-534.
- 472 AMY, L.A. & TALLING, P.J. 2006. Anatomy of turbidite and debrite sandstones based on long  
473 distance (120 x 35 km) bed correlation, Marnoso-arenacea Formation, Northern Appenines,  
474 Italy. *Sedimentology*, **53**, 161-212.
- 475 AMY, L.A., TALLING, P.J., PEAKALL, J., WYNN, R.B. & ARZOLA THYNNE, R.G. 2005. Bed  
476 geometry used to test recognition criteria of turbidites and (sandy) debrites. *Sedimentary*  
477 *Geology*, **79**, 163-174.
- 478 ARNAUD, E., HALVERSON, G.P. & SHIELDS-ZHOU, G. (eds.) 2011. *The Geological Record of*  
479 *Neoproterozoic Glaciations*. Geological Society, London, Memoirs, **36**, 752 p.
- 480 BAAS, J.H. 2000. Duration of deposition from decelerating high-density turbidity currents.  
481 *Sedimentary Geology*, **136**, 71-88.
- 482 BAAS, J.H., BEST, J.L. & PEAKALL, J. 2011. Depositional processes, bedform development and  
483 hybrid flows in rapidly decelerated cohesive (mud-sand) sediment flows. *Sedimentology*, **58**,  
484 1953-1987.
- 485 BENN, D.I. & EVANS, D.J.A. 2010. *Glaciers and Glaciation*. Hodder Education, London, 802 p.
- 486 BINKS, P.J. 1968. *Orroroo Sheet S154-1*. 1:250,000 scale Geological Map and Explanatory Notes,  
487 Primary Industries and Resources South Australia.
- 488 BROOKFIELD, M.E. & MARTINI, I.P. 1999. Facies architecture and sequence stratigraphy in  
489 glacially influenced basins: basic problems and water-level/glacier input-point controls  
490 (with an example from the Quaternary of Ontario, Canada). *Sedimentary Geology*, **123**, 183-  
491 197.
- 492 BUSFIELD, M.E. & LE HERON, D.P. 2013. Glacitectonic deformation in the Chuos Formation of  
493 northern Namibia: implications for Neoproterozoic ice dynamics. *Proceedings of the*  
494 *Geologists Association*, **124**, 778-789.
- 495 CHEEL, R.J. & LECKIE, D.A. 1993. Hummocky cross-stratification. In: Wright, V.P. (ed.)  
496 *Sedimentology Review*. Wiley Blackwell, London, 103-122.
- 497 COATS, R.P. 1981. Late Proterozoic (Adelaidean) tillites of the Adelaide Geosyncline. In:  
498 HAMBREY, AND M.J., HARLAND, W.B. (eds.) *Earth's Pre-Pleistocene Glacial Record*.  
499 Cambridge University Press, Cambridge, 537-548.

- 500 COATS, R.P. & PREISS, W.V. 1987. Stratigraphy of the Umberatana Group. *In*: PREISS, W.V.,  
501 (ed.) *The Adelaide Geosyncline: Late Proterozoic Stratigraphy, Sedimentation,*  
502 *Palaeontology and Tectonics*. Geological Survey of South Australia, Bulletin 53, 125-210.
- 503 COLLINSON, J.D. & THOMPSON, D.B. 1987. *Sedimentary Structures*, 2<sup>nd</sup> edition. Chapman and  
504 Hall, London.
- 505 CONDON, D.J. & BOWRING, S.A. 2011. A user's guide to Neoproterozoic geochronology. *In*:  
506 ARNAUD, E., HALVERSON, G.P., SHIELDS-ZHOU, G. (eds.) *The Geological Record of*  
507 *Neoproterozoic Glaciations*. Geological Society, London, Memoirs, **36**, 135-149.
- 508 COX, G.M., HALVERSON, G.P., MINARIK, W.G., LE HERON, D.P., MACDONALD, F.A.,  
509 BELLEFROID, E.J. & STRAUSS, J.V. *in press*. Neoproterozoic Iron Formation: an  
510 evaluation of its temporal, environmental and tectonic significance. *Chemical Geology*,  
511 <http://dx.doi.org/10.1016/j.chemgeo.2013.08.002>
- 512 DUKE, W.L., ARNOTT, R.W.C. & CHEEL, R.J. 1991. Shelf sandstones and hummocky cross-  
513 stratification: new insights into a stormy debate. *Geology*, **19**, 625-628.
- 514 DUMAS, S. & ARNOTT, R.W.C. 2006. Origin of hummocky and swaley cross-stratification – the  
515 controlling influence of unidirectional current strength and aggradation rate. *Geology*, **34**,  
516 1073-1076.
- 517 EL-GHALI, M.A.K. 2005. Depositional environments and sequence stratigraphy of the paralic  
518 glacial, para-glacial and postglacial Upper Ordovician siliciclastic deposits of the Murzuq  
519 Basin, SW Libya. *Sedimentary Geology*, **177**, 145-173.
- 520 ETIENNE, J.L., ALLEN, P.A., RIEU, R. & LE GUERROUÉ, E. 2007. Neoproterozoic glaciated  
521 basins: a critical review of the Snowball Earth hypothesis by comparison with Phanerozoic  
522 glaciations. *In*: HAMBREY, M.J., CHRISTOFFERSEN, P., GLASSER, N.F. &  
523 HUBBARD, B. (eds.) *Glacial Sedimentary Processes and Products*. Blackwell Publishing  
524 Ltd., Oxford, 343-399.
- 525 EYLES, N. & JANUSZCZAK, N. 2007. Syntectonic subaqueous mass flows of the Neoproterozoic  
526 Otavi Group, Namibia: where is the evidence of global glaciation? *Basin Research*, **19**, 179-  
527 198.
- 528 FANNING, C.M. & LINK, P.K. 2006. Constraints on the timing of the Sturtian glaciogene event  
529 from southern Australia; i.e. for the true Sturtian. *Geological Society of America Abstracts*  
530 *with Programs*, **38**, no. 7, p. 115.
- 531 FORBES, B.G. 1970. Benda Siltstones. *Geological Survey of South Australia, Quarterly Notes*, **33**,  
532 1-2.
- 533 FORBES, B.G. 1989. *Olary Sheet S154-2*. 1:250,000 scale Geological Map and Explanatory Notes,  
534 Primary Industries and Resources South Australia.
- 535 FORBES, B.G. & COOPER, R.S. 1976. The Pualco Tillite of the Olary region, South Australia.  
536 *Geological Survey of South Australia, Quarterly Notes*, **60**, 2-5.
- 537 GRADSTEIN, F.M., OGG, J.G. & SMITH, A.G. (eds) 2004. *A Geologic Time Scale*. Cambridge  
538 University Press, 589 p.

- 539 HOFFMAN, P.F. & SCHRAG, D.P. 2002. The snowball Earth hypothesis: testing the limits of  
540 global change. *Terra Nova*, **14**, 129-155.
- 541 HOFFMAN, P.F., KAUFMAN, A.J., HALVERSON, G.P. & SCHRAG, D.P. 1998. A  
542 Neoproterozoic snowball Earth. *Science*, **281**, 1342-1346.
- 543 HOWCHIN, W. 1901. Preliminary note on the existence of glacial beds of Cambrian age in South  
544 Australia. *Transactions of the Royal Society of South Australia*, **25**, 10-13.
- 545 HOWCHIN, W. 1908. Glacial beds of Cambrian age in South Australia. *Quarterly Journal of the*  
546 *Geological Society*, **64**, 234-259.
- 547 JOBE, Z.R., LOWE, D.R. & MORRIS, W.R. 2012. Climbing-ripple successions in turbidite  
548 systems: depositional environments, sedimentation rates and accumulation times.  
549 *Sedimentology*, **59**, 867-898.
- 550 JOHNSON, A.M. 1970. *Physical Processes in Geology*. Freeman Cooper, San Francisco, 577 p.
- 551 JOHNSON, H.D. & BALDWIN, C.T. 1996. Shallow clastic seas. In: READING, H.G. (ed)  
552 *Sedimentary Environments*. Blackwell, London, pp. 236-286.
- 553 KENDALL, B., CREASER, R.A. & SELBY, D. 2006. Re-Os geochronology of postglacial black  
554 shales in Australia: constraints on the timing of 'Sturtian' glaciation. *Geology*, **34**, 729-732.
- 555 KIRSCHVINK, J.L. 1992. Late Proterozoic low-latitude glaciation: the snowball Earth. In:  
556 SCHOPF, J.W., AND KLEIN, C. (eds.) *The Proterozoic Biosphere*. Cambridge University  
557 Press, Cambridge, 51-52.
- 558 KNELLER, B.C. & BRANNEY, M.J. 1995. Sustained high-density turbidity currents and the  
559 deposition of thick massive sands. *Sedimentology*, **42**, 607-616.
- 560 KUENEN, P.H. 1966. Experimental turbidite lamination in a circular flume. *The Journal of*  
561 *Geology*, **74**, 523-545.
- 562 KUENEN, P.H. & HUMBERT, F.L. 1969. Grain size of turbidite ripples. *Sedimentology*, **13**, 253-  
563 261.
- 564 LE HERON, D.P. 2012. The Cryogenian record of glaciation and deglaciation in South Australia.  
565 *Sedimentary Geology*, **243-244**, 57-69.
- 566 LE HERON, D.P., COX, G.M., TRUNDLEY, A.E. & COLLINS, A. 2011a. Sea ice-free conditions  
567 during the Sturtian glaciation (early Cryogenian), South Australia. *Geology*, **39**, 31-34.
- 568 LE HERON, D.P., COX, G.M., TRUNDLEY, A.E. & COLLINS, A. 2011b. Two Cryogenian  
569 glacial successions compared: aspects of the Sturt and Elatina sediment records of South  
570 Australia. *Precambrian Research*, **186**, 147-168.
- 571 LE HERON, D.P., BUSFIELD, M.E., LE BER, E. & KAMONA, A.F. 2013. Neoproterozoic  
572 ironstones in northern Namibia: biogenic precipitation and Cryogenian glaciation.  
573 *Palaeogeography, Palaeoclimatology, Palaeoecology*, **369**, 48-57.
- 574 LE HERON, D.P., BUSFIELD, M.E., COLLINS, A.S. *in press*. Bolla Bollana boulder beds: A  
575 Neoproterozoic trough mouth fan in South Australia? *Sedimentology* (2013) doi:  
576 10.1111/sed.12082.

- 577 LEGROS, F. 2002. Can dispersive pressure cause inverse grading in grain flows? *Journal of*  
578 *Sedimentary Research*, **72**, 166-170.
- 579 LINK, P.K. & GOSTIN, V.A. 1981. Facies and paleogeography of Sturtian glacial strata (late  
580 Precambrian), South Australia. *American Journal of Science*, **281**, 353-374.
- 581 LOTTERMOSER, B.G. & ASHLEY, P.M. 2000. Geochemistry, petrology and origin of  
582 Neoproterozoic ironstones in the eastern part of the Adelaide Geosyncline, South Australia.  
583 *Precambrian Research*, **101**, 49-67.
- 584 MAJOR, J.J. & IVERSON, R.M. 1999. Debris-flow deposition: effects of pore-fluid pressure and  
585 friction concentrated at flow margins. *Geological Society of America Bulletin*, **111**, 1424-  
586 1434.
- 587 MALTMAN, A. 1994. *The Geological Deformation of Sediments*. Chapman and Hall, Cambridge,  
588 384 p.
- 589 MAWSON, D. 1941. Middle Proterozoic sediments in the neighbourhood of Copley. *Transactions*  
590 *of the Royal Society of South Australia*, **65**, 304-311.
- 591 MAWSON, D. 1949. Sturt tillite of Mount Jacob and Mount Warren Hastings, north Flinders  
592 Ranges. *Transactions of the Royal Society of South Australia*, **72**, 244-251.
- 593 MAWSON, D. & SPRIGG, R.C. 1950. Subdivision of the Adelaide System. *Australian Journal of*  
594 *Science*, **13**, 69-72.
- 595 MIDDLETON, G.V. & HAMPTON, M.A. 1973. Sediment gravity flows: mechanisms of flow and  
596 deposition. Turbidites and Deep-water Sedimentation, SEPM Pacific Section, Short course  
597 lecture notes, p. 1-38.
- 598 Ó'COFAIGH, C., ANDREWS, J.T., JENNINGS, A.E., DOWDESWELL, J.A., HOGAN, K.A.,  
599 KILFEATHER, A.A. & SHELDON, C. 2012. Glacimarine lithofacies, provenance and  
600 depositional processes on a West Greenland trough-mouth fan. *Journal of Quaternary*  
601 *Science*, **28**, 13-26.
- 602 PEDERSEN, S.A.S. 2012. Glaciodynamic sequence stratigraphy. In: HUUSE, M., REDFERN, J.,  
603 LE HERON, D.P., DIXON, R.J., MOSCARIELLO, A. & CRAIG, J. (eds.) *Glaciogenic*  
604 *Reservoirs and Hydrocarbon Systems*. Geological Society, London, Special Publications,  
605 **368**, 29-51.
- 606 PHILLIPS, E. 2006. Micromorphology of a debris flow deposit: evidence of basal shearing,  
607 hydrofacturing, liquefaction and rotational deformation during emplacement. *Quaternary*  
608 *Science Reviews*, **25**, 720-738.
- 609 POSTMA, G., NEMEC, W. & KLEINSPEHN, K.L. 1988. Large floating clasts in turbidites – a  
610 mechanism for their emplacement. *Sedimentary Geology*, **58**, 47-61.
- 611 POWELL, R.D. & COOPER, J.M. 2002. A glacial sequence stratigraphic model for temperate,  
612 glaciated continental shelves. In: DOWDESWELL, J.A. & O'COFAIGH, C. (eds.) *Glacier-*  
613 *Influenced Sedimentation on High-Latitude Continental Margins*. Geological Society,  
614 London, Special Publications, **203**, 215-244.
- 615 PREISS, W.V. 1987. A synthesis of palaeogeographic evolution of the Adelaide Geosyncline. In:  
616 PREISS, W.V. (ed.) *The Adelaide Geosyncline. Late Proterozoic Stratigraphy*,



- 617 *Sedimentation, Palaeontology and Tectonics*. Geological Survey of South Australia  
618 Bulletin, **53**, 315-409.
- 619 PREISS, W.V. 1993. Neoproterozoic. In: DREXEL, J.F., PREISS, W.V. & PARKER, A.J. (eds.)  
620 *The Geology of South Australia. Volume 1, The Precambrian*. Bulletin 54, Mines and  
621 Energy of South Australia. State Print, South Australia, pp. 170-224.
- 622 PREISS, W.V. 1995. Delamerian Orogeny. In: DREXEL, J.F., AND PREISS, W.V. (eds.) *The*  
623 *geology of South Australia. Vol. 2, The Precambrian*. Geological Survey of South Australia,  
624 Bulletin 54, 45-57.
- 625 PREISS, W.V. 1999. *Parachilna Sheet SH54-13*. 1:250,000 scale Geological Map and Explanatory  
626 Notes, Primary Industries and Resources South Australia.
- 627 PREISS, W.V. 2000. The Adelaide Geosyncline of South Australia and its significance in  
628 Neoproterozoic continental reconstruction. *Precambrian Research*, **100**, 21-63.
- 629 PREISS, W.V., BELPERIO, A.P., COWLEY, W.M. & RANKIN, L.R., 1993. Neoproterozoic. In:  
630 DREXEL, J.F., PREISS, W.V. & PARKER, A.J. (eds.) *The geology of South Australia. Vol.*  
631 *1, The Precambrian*. Geological Survey of South Australia, Bulletin 54, 171-203.
- 632 PREISS, W.V., DYSON, I.A., REID, P.W. & COWLEY, W.M. 1998. Revision of lithostratigraphic  
633 classification of the Umberatana Group. *MESA Journal*, **9**, 36-42.
- 634 PREISS, W.V., GOSTIN, V.A., MCKIRDY, D.M., ASHLEY, P.M., WILLIAMS, G.E. &  
635 SCHMIDT, P.W. 2011. The glacial succession of Sturtian age in South Australia: the  
636 Yudnamutana Subgroup. In: ARNAUD, E., HALVERSON, G.P. & SHIELDS-ZHOU, G.  
637 (eds.) 2011. *The Geological Record of Neoproterozoic Glaciations*. Geological Society,  
638 London, Memoirs, **36**, 752 p.
- 639 PROUST, J.N. & DEYNOUX, M. 1994. Marine to non-marine sequence architecture of an  
640 intracratonic glacially-related basin. Late Proterozoic of the West African platform in  
641 western Mali. In: DEYNOUX, M., MILLER, J.M.G., DOMACK, E.W., EYLES, N.,  
642 FAIRCHILD, I.J. & YOUNG, G.M. (eds) *The Earth's Glacial Record: Facies Models and*  
643 *Geodynamic Evolution*. Cambridge University Press, Cambridge, 121-145.
- 644 SUMNER, E.J., AMY, L. & TALLING, P.J. 2008. Deposit structure and processes of sand  
645 deposition from a decelerating sediment suspension. *Journal of Sedimentary Research*, **78**,  
646 529-547.
- 647 TALLING, P.J., MASSON, D.G., SUMNER, E.J. & MALGESINI, G. 2012. Subaqueous sediment  
648 density flows: depositional processes and deposit types. *Sedimentology*, **59**, 1937-2003.
- 649 YOUNG, G.M. & GOSTIN, V.A. 1988. Stratigraphy and sedimentology of Sturtian glaciogenic  
650 deposits in the western part of the North Flinders Basin, South Australia. *Precambrian*  
651 *Research*, v. 39, p. 151-170.
- 652 YOUNG, G.M., AND GOSTIN, V.A. 1989. An exceptionally thick upper Proterozoic (Sturtian)  
653 glacial succession in the Mount Painter area, South Australia. *Geological Society of America*  
654 *Bulletin*, **101**, 834-845.
- 655 YOUNG, G.M. & GOSTIN, V.A. 1990. Sturtian glacial deposition in the vicinity of the  
656 Yankaninna Anticline, North Flinders Basin, South Australia. *Australian Journal of Earth*  
657 *Sciences*, **37**, 447-458.

658 YOUNG, G.M. & GOSTIN, V.A. 1991. Late Proterozoic (Sturtian) succession of the North  
659 Flinders Basin, South Australia; an example of temperate glaciation in an active rift setting.  
660 *In: Anderson, J.R., Ashley, G.M. (eds.) Glacial Marine Sedimentation: Palaeoclimatic*  
661 *Significance*. Geological Society of America Special Paper, **261**, 207-222.

662

663

664

665

666

667

668

669

670

671

672

673

674

675

676

677

678

679

680

681

682

683

684

685

686

687

688

689 **Figure captions**

690 *Figure 1:* Geological sketch map of the Adelaide Fold Belt, modified after Preiss (1993), showing  
691 location of studied sections. Detailed geological maps of study areas inset; A) Holowilena Creek,  
692 modified after Preiss (1999), B) Oladdie Creek and C) Hillpara Creek modified after Binks (1968).

693 *Figure 2:* Sketch map demonstrates distribution of Sturtian sedimentary deposits and depositional  
694 basins throughout the Adelaide Fold Belt, modified after Preiss et al. (1998). Note location of  
695 Barratta Trough and Yudnamutana Trough, representing the principal depocentres during Sturtian  
696 glaciation.

697 *Figure 3:* Cryogenian stratigraphy and geochronology of the Adelaide Fold Belt and Stuart Shelf,  
698 after Preiss et al. (1998). Note disparity in stratigraphic nomenclature of ‘Sturtian’ glacial  
699 deposits across South Australia. In this paper data are presented from the Yudnamutana Subgroup  
700 of the central and south-west Flinders Ranges.

701 *Figure 4:* Logged sections of the Yudnamutana Subgroup in the central and southern Flinders  
702 Ranges; A) Holowilena Creek (base of log: 31°59.232’S 138°51.052’E), B) Oladdie Creek (base of  
703 log: 32°28.039’S 138°38.285’E), C) Hillpara Creek (base of log: 32°33.777’S 138°47.302’E). Note  
704 the variable thickness and lateral distribution of the five facies associations across the logged  
705 sections. Significant thickness changes from north to south attest to irregular palaeotopographic  
706 relief during deposition.

707 *Figure 5:* Representative photographs of the diamictite and conglomerate facies association. (a)  
708 Erosive scour at base of normally-graded conglomerate-sandstone interbeds (white triangles  
709 demonstrate grading patterns); (b) Ice-rafted dropstone, puncturing and downwarping the  
710 underlying laminae. Compaction related deflection above lonestone significantly lower in amplitude  
711 than below; (c) Ice-rafted debris with impact related deformation; (d-e) Profile view of rotational  
712 turbate structures (circular alignment of clasts around a core stone or rigid matrix). Coin and lens  
713 cap for scale measure 2 cm and 5 cm, respectively.

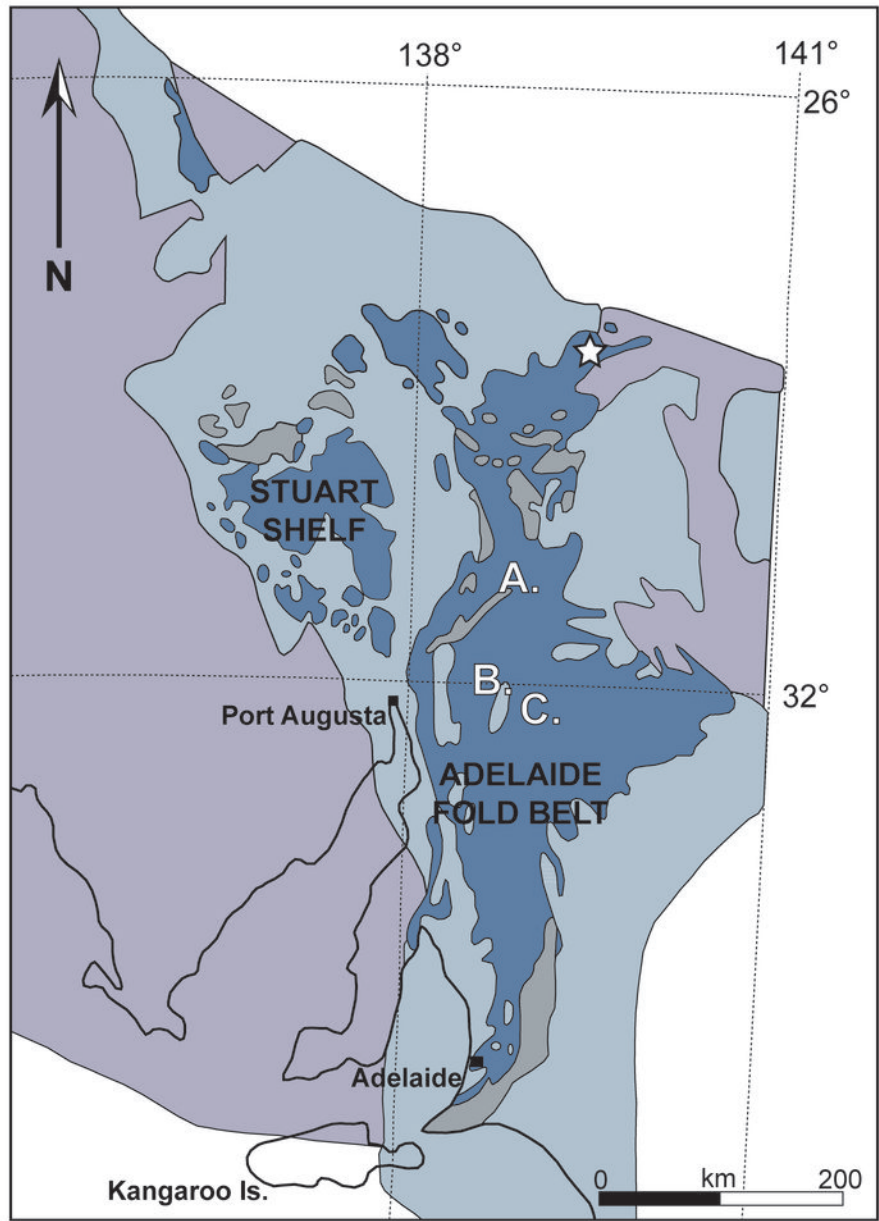
714 *Figure 6:* **Interbedded heterolithic facies association:** (a) Fine-grained current ripple cross-  
715 laminated sandstone and coarse to granule erosive based sandstone interbeds; (b) Soft-sediment  
716 slump folded sandstone interbeds; (c) Trough cross-lamination, convolute laminae and load and  
717 flame structures in beds which onlap the underlying Pualco Tillite (see Fig. 8a). **Hummocky cross-**  
718 **stratified sandstone facies association:** (d) Dominantly isotropic hummocky cross-stratified  
719 sandstone interbeds, interpretive overlay in (e); (f) Amalgamated sets of isotropic cross strata, with  
720 truncation of laminae to the left and above coin. **Lonestone-bearing siltstone facies association:**  
721 (g) ice-rafted debris downwarps and punctures underlying silt. **Ferruginous siltstone and**  
722 **sandstone facies association:** (h) Distinct, sharp banding within the Holowilena Ironstone  
723 interpreted as possible algal laminites. Note irregular fold structure/possible domed algal laminite,  
724 verging towards the south-east. (i) Micro-scale ice-rafted debris which punctures and downwarps  
725 underlying laminae. Coin for scale measures 2 cm.

726 *Figure 7:* Sequence stratigraphic framework for the studied sections. Glacial systems tracts are  
727 separated either by a glacial erosion surface (GES) or glacial bounding surface (GBS), the latter  
728 including the glacial advance surface (GAS) and iceberg-rafting termination surface (ITS). Key for  
729 glacial systems tracts codes: **GAST**= glacial advance systems tract; **GRST**= glacial retreat systems  
730 tract; **GMAST**= glacial maximum systems tract; **GMiST**= glacial minimum systems tract.

731 *Figure 8:* Photographs of significant depositional boundaries within the studied succession. (a)  
732 Glacially-influenced Pualco Tillite onlapped by non-glacially influenced interbedded heterolithics

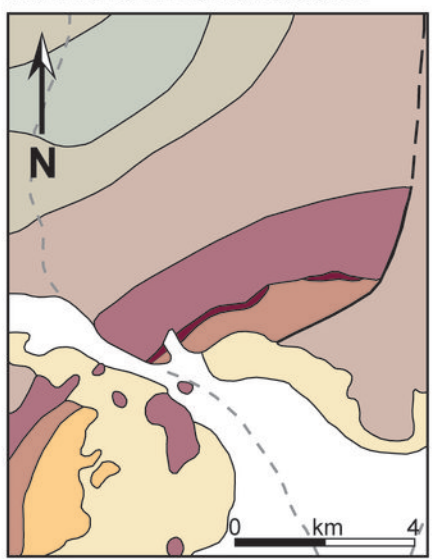
733 (see Fig. 6c); (b) Glacial erosion surface at the base of the Wilyerpa Formation, downcutting into  
734 the Holowilena Ironstone; (c) Influx of extrabasinal granite clasts, indicated by white arrows, at  
735 inferred glacial maximum; (d) Conglomeratic transgressive lag records terminal glacial conditions  
736 at the top of the Wilyerpa Formation, succeeded by post-glacial siltstone of the Tapley Hill  
737 Formation. Hammer and lens cap for scale measure 26 cm and 5 cm, respectively.

738 *Figure 9:* Simple depositional model for the studied sections in the central and southern Flinders  
739 Ranges. Sequence stratigraphic analysis identifies four glacial advance sequences, separated by  
740 three intervals of ice meltback. During glacial advance, dynamic ice sheet oscillations drive  
741 delivery of glaciogenic debris flows and glacioturbidites downslope, subject to secondary ice-  
742 rafting. During glacial retreat, the ice-rafting signature is lost, and ice minimum conditions permit  
743 storm-wave agitation of the water column, and generation of hummocky cross-stratified sandstones.  
744 Thickness variations across the logged sections attest to significant palaeotopographic relief during  
745 deposition, creating progressively greater accommodation space downslope (Hillpara-Oladdie-  
746 Holowilena) through the combined effects of pre- and early syn-depositional rift activity and  
747 subglacial downcutting. Key for glacial systems tracts codes: **GAST**= glacial advance systems tract;  
748 **GRST**= glacial retreat systems tract; **GMaST**= glacial maximum systems tract; **GMiST**= glacial  
749 minimum systems tract.

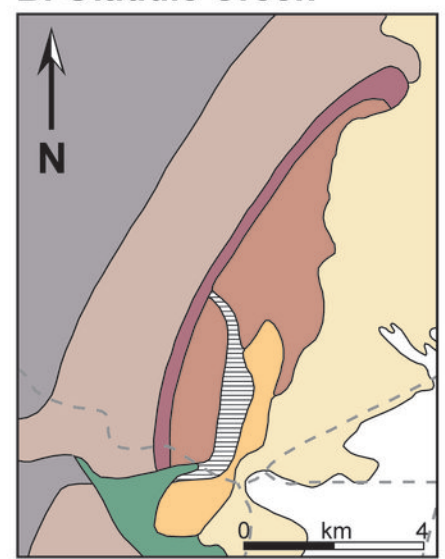


- Cambrian rocks
- Neoproterozoic (Adelaidian: outcrop)
- Pre-Neoproterozoic rocks
- Neoproterozoic (Adelaidean: subsurface)
- ☆ Bolla Bollana Trough Mouth Fan

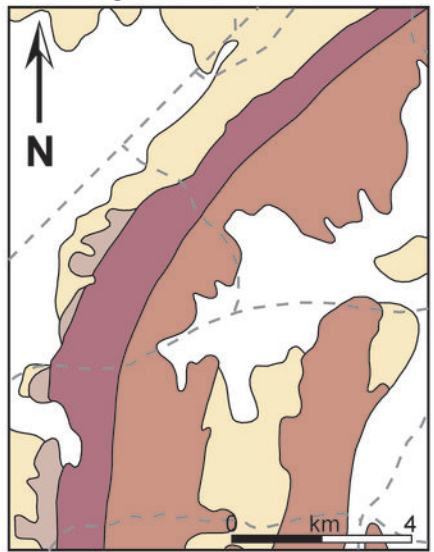
**A. Holowilena South**



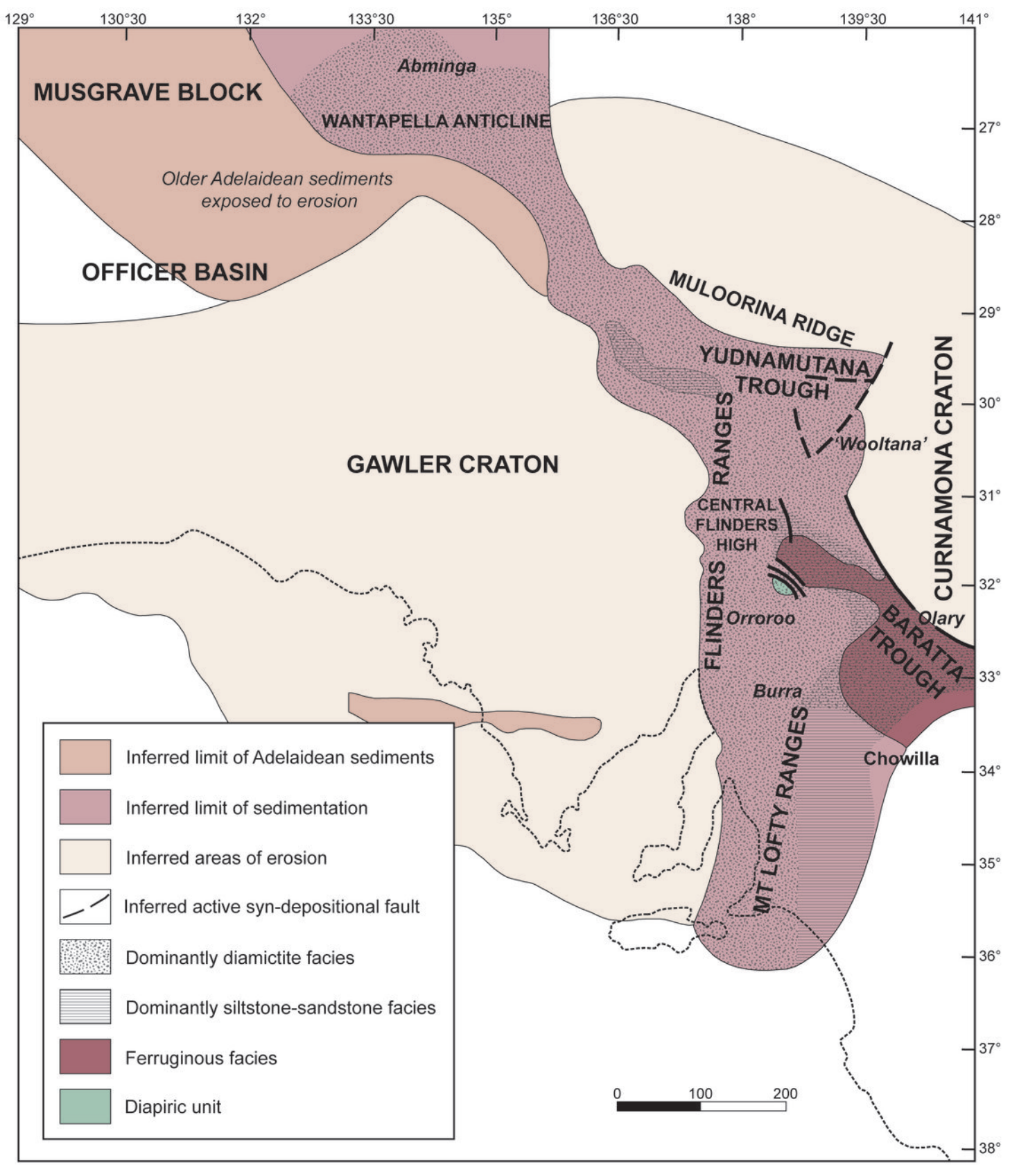
**B. Oladdie Creek**

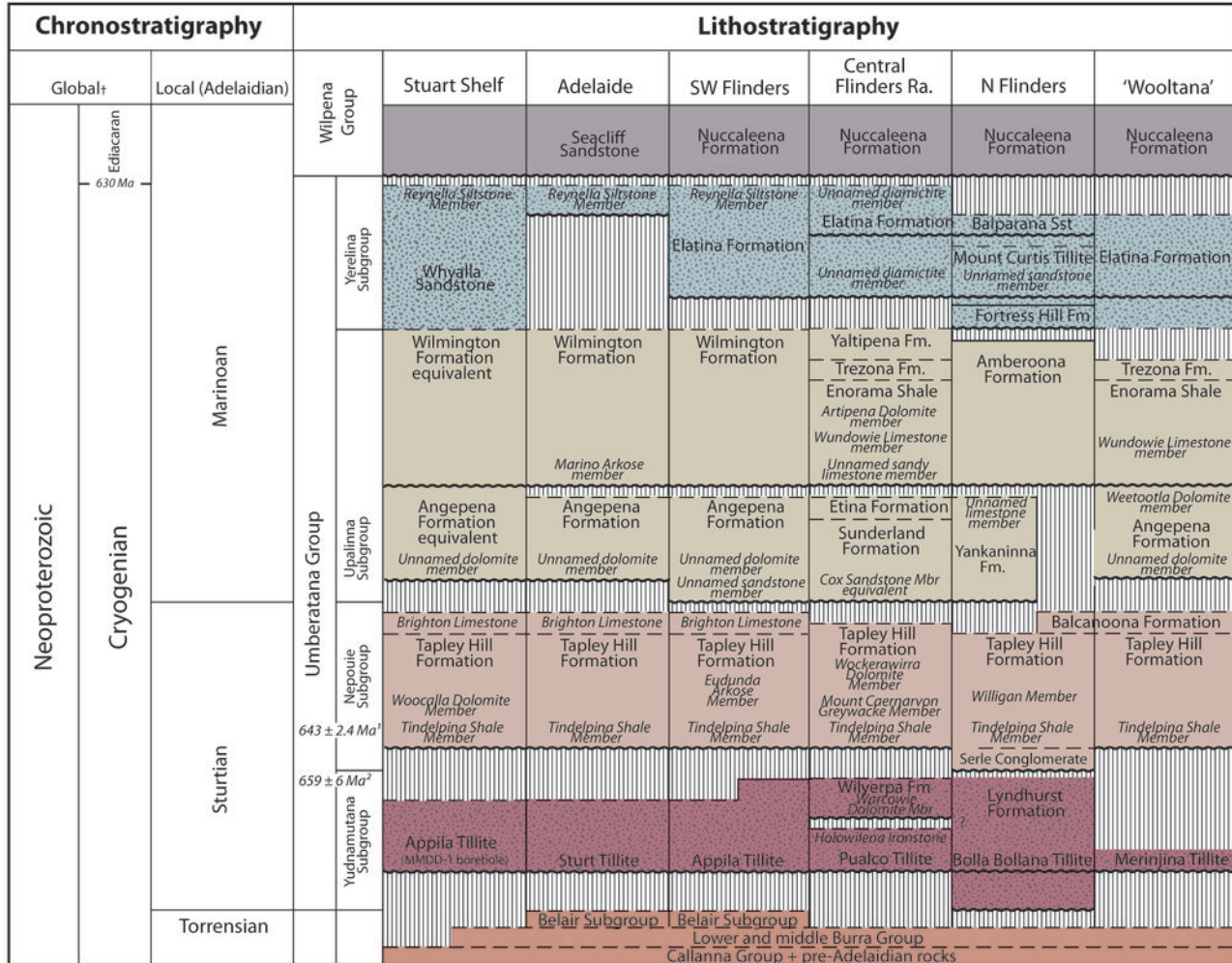


**C. Hillpara Creek**



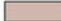



- Pleistocene cover
  - Wilpena Group
  - Enorama Shale
  - Etina Formation
  - Tapley Hill Formation
  - Wilyerpa Formation
  - Holowilena Ironstone
  - Burra Group
  - River Wakefield Group
  - Diapiric Breccia
  - Crush zone
  - Fault
  - Track
- Yudnamutana Subgroup**





### LEGEND

-  Hiatus
-  Marinoan glacial deposits
-  Sturtian post-glacial deposits
-  Sturtian glacial deposits

### NOTES

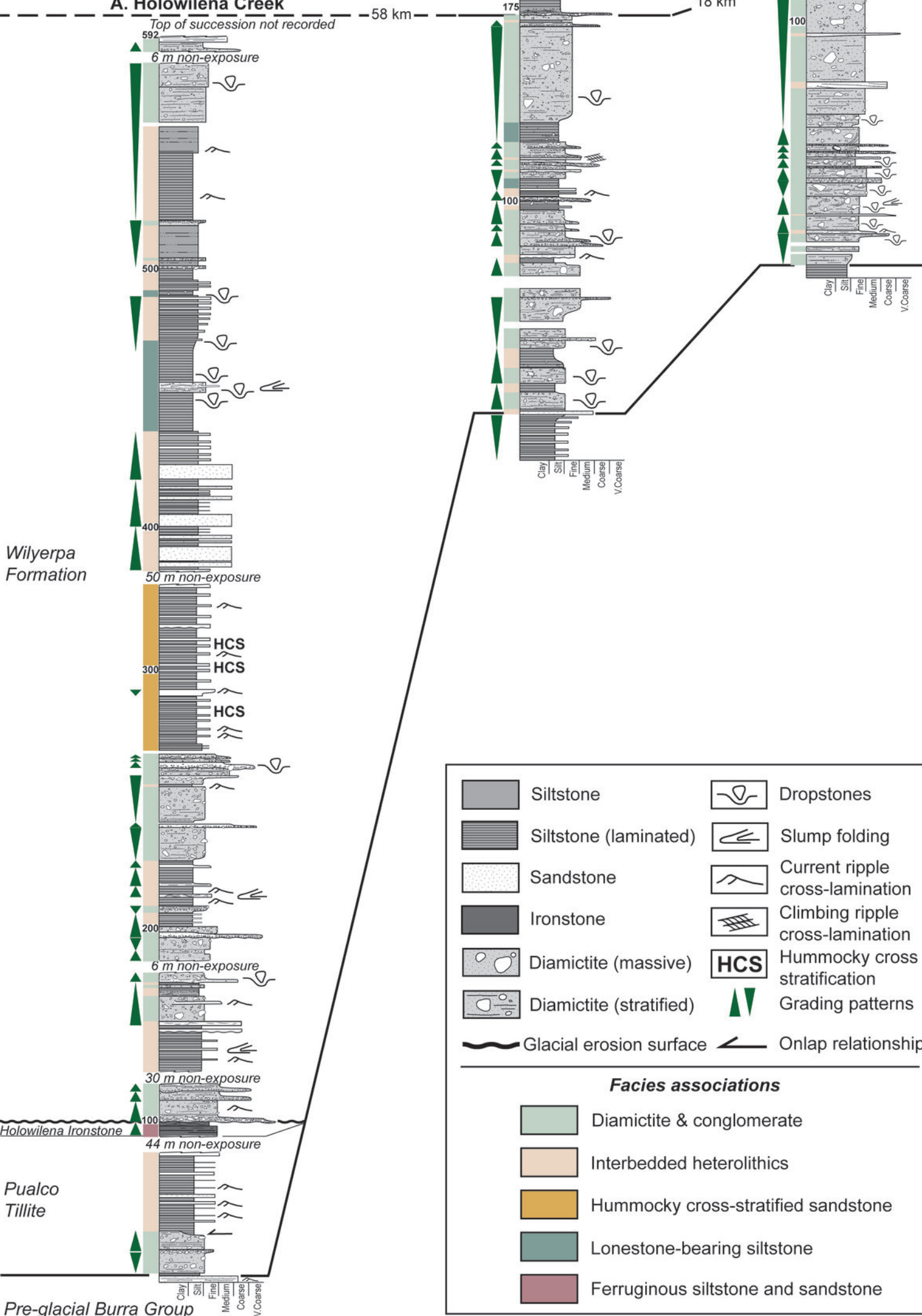
- †Gradstein et al. (2004)
- <sup>1</sup>Re-Os date: basal Tindelpina Shale Mbr (Kendall et al., 2006)
- <sup>2</sup>U-Pb date: top Wilyerpa Fm (Fanning & Link, 2006)

Post-glacial Tapley Hill Formation

**A. Holowilena Creek**

**B. Oladdie Creek**

**C. Hillpara Creek**



Wilyerpa Formation

Pualco Tillite

Pre-glacial Burra Group

Top of succession not recorded  
592  
6 m non-exposure  
500  
400  
50 m non-exposure  
300  
HCS  
HCS  
HCS  
200  
6 m non-exposure  
100  
30 m non-exposure  
100  
44 m non-exposure

175  
100  
Clay  
Silt  
Fine  
Medium  
Coarse  
V.Coarse

Top not recorded  
100  
Clay  
Silt  
Fine  
Medium  
Coarse  
V.Coarse

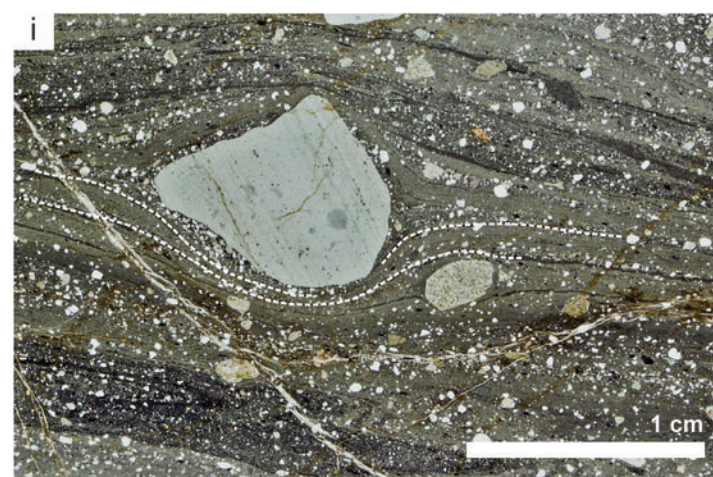
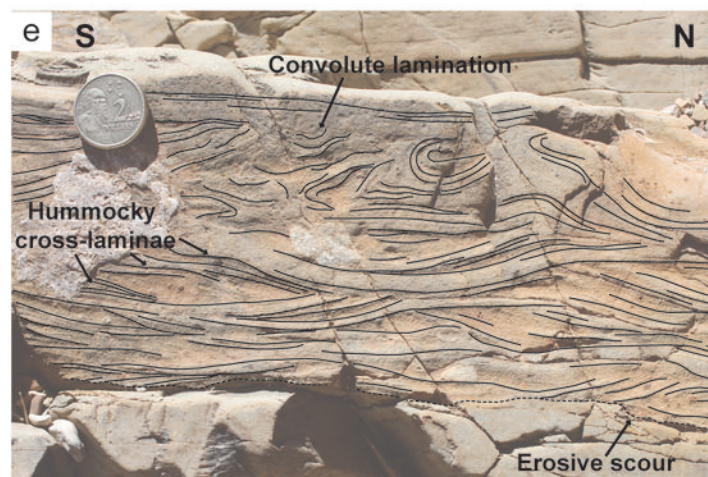
- Siltstone
- Siltstone (laminated)
- Sandstone
- Ironstone
- Diamictite (massive)
- Diamictite (stratified)
- Dropstones
- Slump folding
- Current ripple cross-lamination
- Climbing ripple cross-lamination
- Hummocky cross stratification
- Grading patterns
- Glacial erosion surface
- Onlap relationship

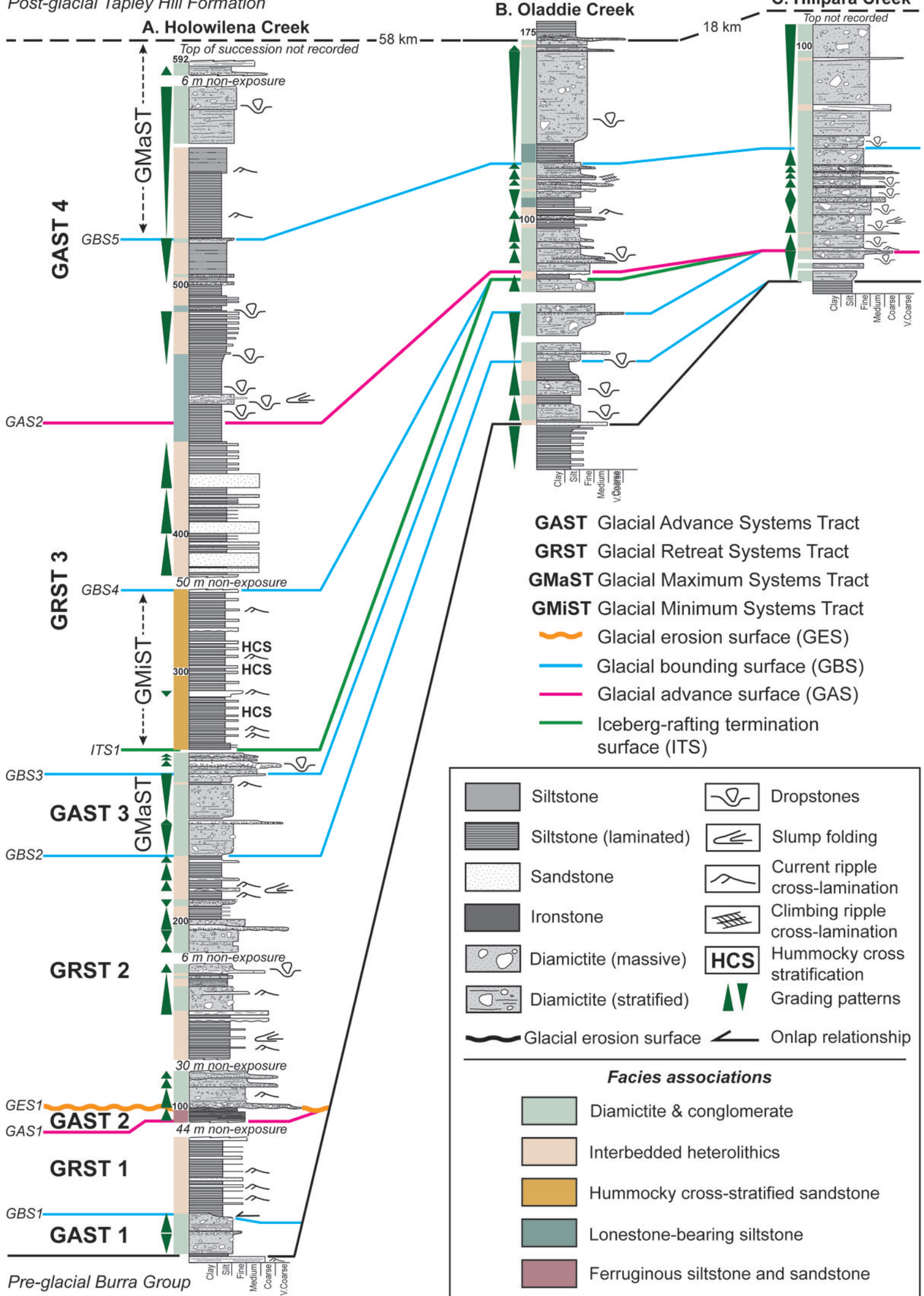
**Facies associations**

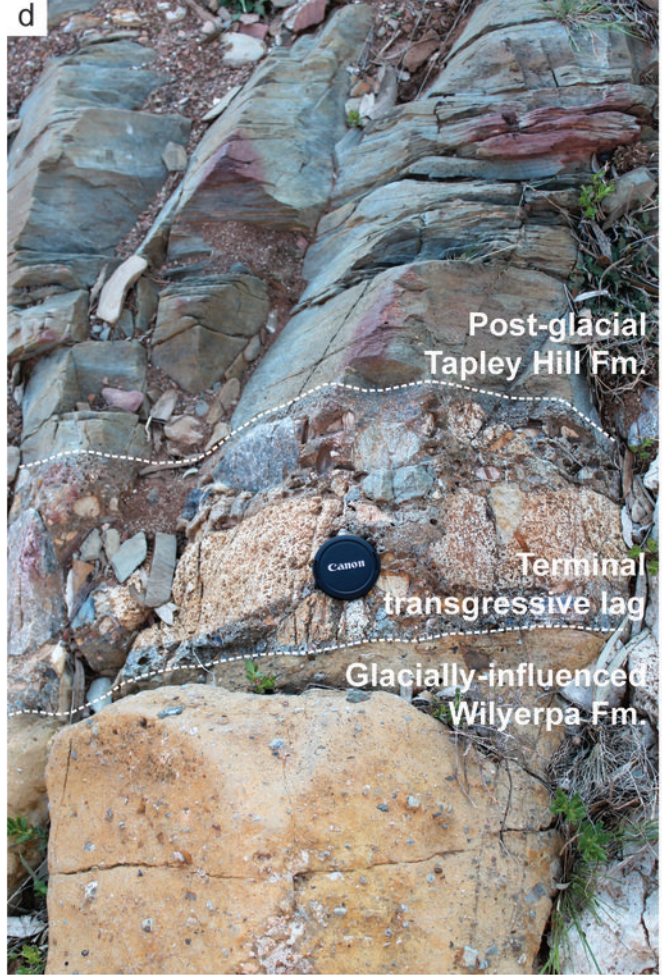
- Diamictite & conglomerate
- Interbedded heterolithics
- Hummocky cross-stratified sandstone
- Lonestone-bearing siltstone
- Ferruginous siltstone and sandstone

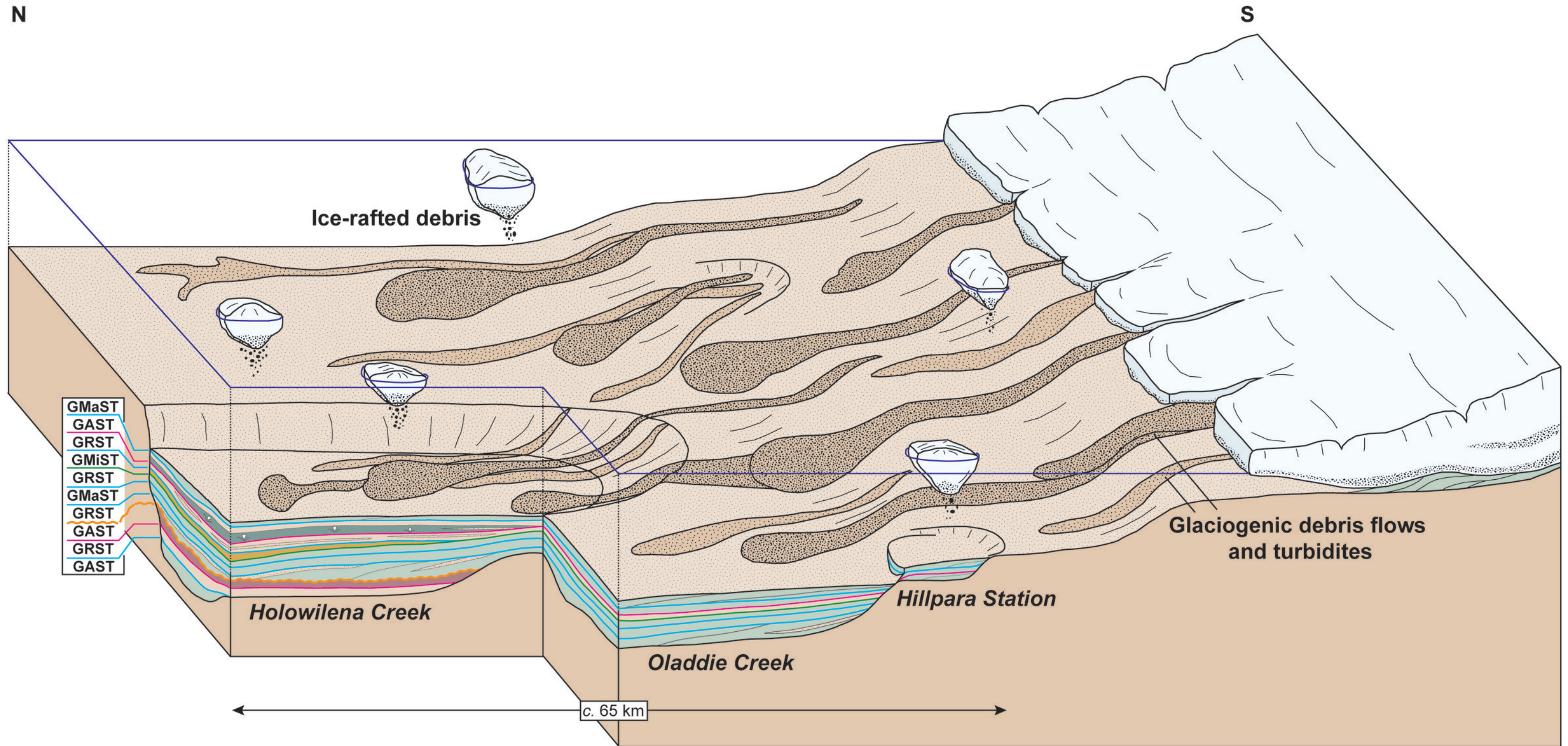












**Sequence boundaries**

— Glacial bounding surface (GBS)    
 — Glacial erosion surface (GES)    
 — Glacial advance surface (GAS)    
 — Iceberg-rafting termination surface (ITS)

**Facies associations**

<span style="display: inline-block; width: 20px; height: 10px; background-color: #c8e6c9; border: 1px solid black;"></span> Diamictite & conglomerate	<span style="display: inline-block; width: 20px; height: 10px; background-color: #e0e0e0; border: 1px solid black;"></span> Interbedded heterolithics	<span style="display: inline-block; width: 20px; height: 10px; background-color: #f1c40f; border: 1px solid black;"></span> Hummocky cross-stratified sandstone	<span style="display: inline-block; width: 20px; height: 10px; background-color: #808080; border: 1px solid black;"></span> Lonestone-bearing siltstone	<span style="display: inline-block; width: 20px; height: 10px; background-color: #a52a2a; border: 1px solid black;"></span> Ferruginous siltstone and sandstone
---	---	---	---	---